Anthropogenic Contaminants Shape the Fitness of the Endangered European Eel: A Machine Learning Approach

Bastien Bourillon, Eric Feunteun, Anthony Acou, Thomas Trancart, Nils Teichert, Claude Belpaire, Sylvie Dufour, Paco Bustamante, Kim Aarestrup, Alan Walker, et al.

fishes

MDPI

Article

Anthropogenic Contaminants Shape the Fitness of the Endangered European Eel: A Machine Learning Approach

Bastien Bourillon [1,†], Eric Feunteun [1,2,*,†], Anthony Acou [3], Thomas Trancart [1], Nils Teichert [1], Claude Belpaire [4], Sylvie Dufour [5], Paco Bustamante [6,7], Kim Aarestrup [8], Alan Walker [9] and David Righton [9]

1 Laboratoire Biologie des Organismes et Ecosystèmes Aquatiques (BOREA), Muséum National d'Histoire Naturelle, UMR 8067 CNRS, Centre de Recherche et d'Enseignement sur les Systèmes Côtiers, station de biologie marine de Dinard, Sorbonne Université, IRD 207, Université de Caen Normandie, Université des Antilles, 38 rue du Port Blanc, 35800 Dinard, France
2 EPHE-PSL, Centre de Géoécologie Littorale, Boulevard de la mer, 35800 Dinard, France
3 UAR OFB-CNRS-MNHN PatriNat, Station de Biologie Marine de Dinard, 38 rue du Port Blanc, 35800 Dinard, France
4 Research Institute for Nature and Forest (INBO), Dwersbos 28, 1630 Linkebeek, Belgium
5 Laboratoire Biologie des Organismes et Ecosystèmes Aquatiques (BOREA), Muséum National d'Histoire Naturelle, CNRS UMR 8067, Sorbonne Université, IRD 207, Université de Caen Normandie, Université des Antilles, 43 rue Cuvier, CEDEX 5, 75231 Paris, France
6 Littoral, Environnement et Sociétés (LIENSs), UMR 7266 CNRS, La Rochelle Université, 2 rue Olympe de Gouges, 17000 La Rochelle, France
7 Institut Universitaire de France (IUF), 1 rue Descartes, 75005 Paris, France
8 DTU AQUA, National Institute of Aquatic Resources, Section for Freshwater Fisheries Ecology, Technical University of Denmark, Vejlsøvej 39, 8600 Silkeborg, Denmark
9 Centre for Environment, Fisheries and Aquaculture Science, Pakefield Road, Lowestoft, Suffolk NR33 0HT, UK
* Correspondence: eric.feunteun@mnhn.fr
† These authors contributed equally to this work.

Abstract: European eel is thought to be a symbol of the effects of global change on aquatic biodiversity. The species has persisted for millions of years and faced drastic environmental fluctuations thanks to its phenotypic plasticity. However, the species has recently declined to historically low levels under synergistic human pressures. Sublethal chemical contamination has been shown to alter reproductive capacity, but the impacts and required actions are not fully addressed by conservation plans. This paper proposes a modelling approach to quantify the effects of sublethal contamination by anthropogenic pollutants on the expression of life history traits and related fitness of the critically endangered European eel. **Material and Methods**: We sampled female silver eels from eight different catchments across Europe previously shown to be representative of the spectrum of environmental variability and contamination. We measured 11 fitness-related life history traits within four main categories: fecundity, adaptability and plasticity, migratory readiness, and spawning potential. We used machine learning in models to explore the phenotypic reaction (expression of these life history traits) according to geographical parameters, parasite burdens (the introduced nematode *Anguillicoloides crassus*) and anthropogenic contaminants (persistent organic pollutants (POPs) in muscular tissue and trace elements (TEs) in gonads, livers and muscles). Finally, we simulated, the effects of two management scenarios—contamination reduction and contamination increase—on the fecundity and recruitment. **Results**: Contamination in our sampling was shown to have a stronger control on life history traits than do geographic and environmental factors that are currently described in the literature. We modelled different contamination scenarios to assess the benefit of mitigation: these scenarios suggest that reducing pollutants concentrations to the lowest values that occurred in our sampling design would double the fecundity of eels compared to the current situation. **Discussion**: Remediation of contamination could represent a viable management option for increasing the resilience of eel populations, with much more effects than solely reducing fishing mortality. More broadly, our work provides an innovative way for quantitative assessment of the reaction norms of species' biological traits and related fecundity to contamination by organic and

check for updates

Citation: Bourillon, B.; Feunteun, E.; Acou, A.; Trancart, T.; Teichert, N.; Belpaire, C.; Dufour, S.; Bustamante, P.; Aarestrup, K.; Walker, A.; et al. Anthropogenic Contaminants Shape the Fitness of the Endangered European Eel: A Machine Learning Approach. *Fishes* **2022**, *7*, 274. https://doi.org/10.3390/fishes7050274

Academic Editor: Wann-Nian Tzeng

Received: 12 September 2022
Accepted: 29 September 2022
Published: 5 October 2022

Publisher's Note: MDPI stays neutral with regard to jurisdictional claims in published maps and institutional affiliations.

inorganic pollutions thus opening new management and conservation pathways to revert the erosion of biodiversity.

Keywords: life history traits; global change; biogeography; Anguilla

1. Introduction

Since their emergence approximately 60–70 million years ago, anguillid eels have outlived the dinosaurs, adapted to continental shifts, survived oceanographic regime shifts and glaciation events [1]. Anguillid eels have successfully colonized all continents except Antarctica but their species diversity remained limited (19 species and subspecies) [2,3]. This Genus' evolutionary resilience appears due to the adaptability inherent in their unique life-cycle. All eels begin life in the tropical ocean, where eggs hatch into leptocephalus larvae that migrate on currents towards continental shelves [4]. Leptocephali metamorphose into glass eels [4], and then migrate to coastal, brackish and inland waters where they grow as yellow eels for up to several decades [5]. Finally, they metamorphose into silver eels and become sexually mature as they migrate back to the oceanic spawning areas to breed and die [5]. A critical element is that the silvering is delayed if eels have not reached a minimum size and fat content, which is dependent upon conditions experienced during the growth phase [6–9]. This phenotypic plasticity optimizes the trade-off for individuals between fecundity and mortality, and may be an evolutionary response to environmental heterogeneity [10,11].

Despite their individual adaptive resilience, populations of eels worldwide have drastically declined since the 1980s, and 13 species are classified by IUCN as 'near threatened' or above [12]. Declines have been attributed to a broad cumulative range of anthropogenic activities [13–15]. Globally, shifts of oceanographic regime and food webs due to the ocean warming may affect the survival and migration of eel larvae and glass eels [14]. Regionally and locally, impacts on freshwater ecosystems through hydrological modification and exploitation reduces habitat quality [15,16], while the accelerating development of dams and weirs since the 1950s has created barriers to migration that reduce habitat quantity [17]. Direct reduction in population size occurs through fishing, hydroelectric turbines and accidental spills of toxic contaminants [14,18]. Indirect mortality, or physiological impairments, have been demonstrated for some species due to introduced pathogens [19] or through chronic contamination by organic and trace elements [18,20–26].

The European eel (*Anguilla anguilla*) is the only anguillid eel species classified as 'critically endangered' [12]. Glass eel recruitment in the early part of the 21st century was 5% of the levels reported from the 1970s [27]. Therefore, the European Union implemented a long-term management plan in 2007 to restore the biomass of silver eels that escape to spawn to at least 40% of the biomass that would have been produced under pristine conditions. Subsequently, efforts have focused on reducing fisheries mortality, increasing recruitment through restocking and improving population productivity through habitat restoration [28]. However, there are no clear signs of eel stocks recovery [27], and stronger management measures may be required [12,29]. One aspect yet unexplored is accounting for, or the mitigation of, chronic and sublethal contamination. Many laboratory studies demonstrated the impacts of pollution on eel physiology [18,20–26], but the consequences on population level remain poorly understood because many of these effects occur during sexual maturation and spawning migration, when eels are inaccessible to researchers [29].

At present, the most effective way to assess impacts of contamination on the reproductive stage is to sample female silver eels at the start of their spawning migration [30]. Females are significantly larger than males, and represent the majority of the spawning biomass [5]. During sexual maturation, contaminants appear to be transferred from somatic cells to oocytes [31,32], which represents a threat to egg and embryo development [21].

The aim of our research is to propose an innovative method to quantify the effect of contamination cocktails on the fitness of an endangered species that is submitted to an important fishery. In order to achieve this, we modelled the effects of contamination on various life history traits, including fecundity of females and resulting production of glass eels, thus enabling to compare a loss off glass eel recruitment due to contamination and fisheries.

To this end, we tested the effects of contamination on life history traits of silver eel females from eight different catchments across Europe previously shown to be representative of the spectrum of environmental variability and contamination [33]. We used machine learning in models to explore the expression of 11 life history traits (LHTs) according to geographical parameters, parasite burdens and anthropogenic contaminants (persistent organic pollutants (POPs) in muscular tissue and trace elements (TEs) in gonads, livers and muscles). Finally, we developed a simple model to estimate the effects of fecundity surrogate traits on the production of young recruits, the so called glass eels to compare the effects of "quality improvement" with "fishery control" management measures. To finish we discuss on the transferability of such life history based approach conducted on an iconic largely spread species to estimate the effects of sublethal contamination on the erosion of biodiversity.

2. Methods

2.1. Data Origin

Most data were collected within the national Belgian and European (EELIAD) eel sampling programs [34]. The data in the present study are a subsample of a dataset already used to map the silver eels quality (i.e., lipid content, muscular contaminations and *A. crassus* abundance) [33]. The dataset demonstrated the character and pattern of eel quality in each studied catchment using a representative sample of eels. We have supplemented these data in the current analysis through the collection of new data on contaminations and life history traits (LHTs) from a subset of the eels described in Bourillon et al. [33]. In doing so, we assume that the eel samples used in our new study are representative of their catchment and of the broad spectrum of quality that exists in rivers across Europe.

2.2. Eel Sampling

We captured 331 silver eels at the start of their migration in 2009–2010 from eight catchments across Europe between 43° and 58° north (Figure 1, Table 1). We used a length stratified sampling protocol to catch eels of at least 45 cm in length with a set of passive gears and electrofishing. For the quality analysis we subsampled 75 female silver eels, on average, 9–10 eels per catchment that were representative of the size spectrum of each site.

Table 1. Details of sampling sites.

ID	Country	Sampling Site	Latitude	Longitude	Area (km^2)	Waterbody Type	Salinity	Sampling Gear	Sampling Date (m/d/y)
swSTO	Sweden	Stockholm archipelago	58°57′30.82″	18°02′05.09″	467	S	BW	A	10/12/2009
deGUD	Denmark	Gudenå	55°58′01.31″	09°42′16.64″	2684	R	FW	B	11/12 to 12/14/2009
irCOR	Ireland	Corrib	53°16′32.05″	09°03′21.71″	3167	Cr + L	FW	C	11/16/2009
ukWAR	U.K.	Warwickshire Avon	52°10′00.46″	01°47′27.39″	4588	R	FW	B	11/05/2009
beSCH	Belgium	Scheldt	51°03′58.53″	04°23′19.97″	20,282	R + Cp	FW	D + E	10/19 to 10/27/2009
frFRE	France	Frémur	48°34′39.80″	02°06′13.1″	60	Cr	FW	B	01/19 to 03/01/2010
frLOI	France	Loire	47°22′59.80″	00°50′07.1″	116,962	R	FW	F	12/09 to 12/26/2009
frBAG	France	Bages-Sigean	43°03′39.61″	02°59′38.06″	411	Lg	BW	D	11/08 to 12/16/2009

Waterbody type: Cp = canals and ponds, Cr = coastal river, L = lake system, Lg = lagoon, R = river, S = Baltic sea. Salinity: BW = brackish water, FW = freshwater. Sampling gear: A = pound net, B = eel trap, C = Coghill net, D = fyke net, E = electrofishing, F = trap net leaders.

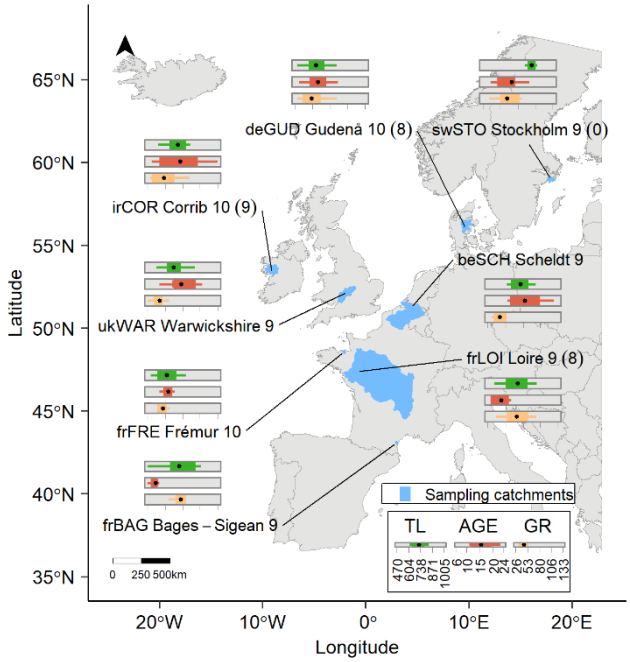

Figure 1. Sampling sites throughout Europe. For each catchment, the identifier (related to Table 1), the full name, the number of eels (in brackets: number of eels for the 11-ketotestoterone trait, if different) and the boxplots of total length (TL, mm), age (year) and growth rate (GR, mm·year^{-1}) are displayed. Catchment area is displayed by blue shading.

2.3. Biometry and Dissection

Each institution involved in the sampling anesthetized and euthanized the eels according to their national ethical standards [33]. We anaesthetized eels and measured their total length (TL, mm), total weight (TW, g), and the horizontal (A, mm) and vertical (B, mm) eyes diameters were measured with a slide caliper. After euthanasia and decapitation, blood was immediately sampled (1 mL) from 62 eels with needle from the aorta for 11-ketotestosterone assay. The blood was directly centrifuged at 5000 rotation per minutes for three minutes to separate the plasma, which was then frozen at −80 °C. We dissected the individuals and collected the gonads, samples of dorso-ventral muscles, swimbladder, digestive tract and liver, weighed (in g) and froze all the samples at −20 ° C except the swimbladder.

2.4. Lipids, Contaminants and Parasitism

The experimental protocols were published in a previous article [33] and summarised in Supplementary Table S1. Briefly, muscle samples were used for assaying the concentration of lipid (expressed in %) by gravimetric methods, the concentration of mercury by atomic absorption spectrophotometer, and the concentrations of a further 12 trace elements (TEs, with As, Cd, Co, Cr, Cu, Fe, Hg, Mn, Ni, Pb, Se, and Zn, expressed as μg·g^{-1} dry weight) and a suite of persistent organic pollutants (POPS, expressed as ng·g^{-1} wet weight) by mass spectrometry. We also measured trace elements in the gonads and livers. A total of 63 POPs were analysed and classed into six groups: DDTs (including five dichlorodiphenyltrichloroethane isomers and metabolites: p,p′-DDT, o,p′-DDT, p,p′-DDD, o,p′-DDD, and p,p′-DDE), the HCB (hexachlorobenzene), the BTBPE [1,2-bis (2,4,6-tribromophenoxy)ethane], three HBCDs isomers (α-, β-, and γ-hexabromocyclododecanes), 13 PBDEs (polybromodiphenyls, #IUPAC (International Union of Pure and Applied Chemistry): 28, 47, 49, 66, 85, 99, 100, 153, 154, 183, 196, 197, and 203) and 40 PCBs congeners (polychlorinated biphenyls, #IUPAC: 18, 28, 31, 44, 47, 49, 52, 66, 74, 87, 95, 99, 101, 105, 110, 118, 128, 132, 138, 146, 149, 151, 153, 156, 157, 170, 171, 172, 174, 177, 180, 183, 187, 194, 195, 196, 199, 203, 206, and 209). We opened the swimbladder lumen, made observations using an optical stereomicroscope and counted the abundance of the *A. crassus* nematode.

2.5. Life History Traits

We selected 11 life history traits (LHTs) that, together, integrate the probability and success of eel reproduction [30,35–44] (Table 2). The measurement of fitness-related traits was based on both morphometric data and laboratory analyses: TL (mm), TW (g), continental growth rate (GR, mm·year^{-1}), residence time (AGE, in year), body condition (K), 11-ketotestoterone concentration in plasma (P11KT, pg·mL^{-1}), ocular index (OI, %), digestive tract index (DTI, %), gonado-somatic index (GSI, %), muscular lipid reserves (LIPIDS, %) and the reproductive potential index (RP, g of eggs).

Table 2. Distribution of fitness-related traits of female silver eels by sampled catchments.

Traits Groups	Traits	Catchments							
		swSTO ***n* = 9 (0)**	**deGUD** ***n* = 10 (8)**	**irCOR** ***n* = 10 (9)**	**ukWAR** ***n* = 9**	**beSCH** ***n* = 9**	**frFRE** ***n* = 10**	**frLOI** ***n* = 9 (8)**	**frBAG** ***n* = 9**
Fecundity	TL	843.6 (51.1)	628.2 (91.4)	700.9 (133.9)	667.0 (94.5)	719.1 (75.9)	614.8 (88.4)	698.3 (150.9)	710.4 (137.5)
		754.0–929.0	486.0–787.0	482.0–970.0	538.0–833.0	616.0–837.0	495.0–763.0	522.0–1005.0	470.0–875.0
	TW	1221.6 (167.4)	488.0 (193.4)	689.1 (401.9)	575.6 (290.7)	533.6 (169.0)	437.0 (217.9)	736.0 (686.0)	712.4 (438.2)
		1001.8–1541.2	222.0–849	174.0–1627.0	279.8–1204.3	343.2–924.7	208.9–929.2	195.0–2420.0	164.8–1381.7
Adaptability and plasticity	GR	62.7 (16.9)	51.2 (19.4)	50.6 (20.4)	43.9 (13.5)	44.3 (8.3)	49.1 (9.4)	69.6 (20.2)	82.9 (22.5)
		36.1–86.1	30.0–89.4	30.4–89.7	26.3–69.1	32.0–54.3	40.9–69.8	38.1–99.6	57.9–133.2
	AGE	13.4 (4.4)	11.9 (3.0)	14.4 (6.1)	14.6 (3.8)	15.4 (4.4)	11.3 (1.3)	9.4 (1.9)	8.0 (1.8)
		8.0–22.0	7.0–17.0	7.0–24.0	9.0–20.0	11.0–23.0	9.0–13.0	7.0–12.0	6.0–12.0
	K	0.2 (0.02)	0.2 (0.0)	0.2 (0.0)	0.2 (0.0)	0.1 (0.0)	0.2 (0.0)	0.2 (0.0)	0.2 (0.0)
		0.2–0.2	0.2–0.2	0.2–0.2	0.2–0.2	0.1–0.2	0.2–0.2	0.1–0.2	0.1–0.2
Migratory readiness	P11KT	-	79.0 (24.3)	203.8 (82.0)	71.5 (46.7)	74.7 (35.0)	74.0 (38.3)	218.2 (62.9)	190.0 (130.0)
		-	47.0–114.1	82.6–318.0	13.1–157.4	16.1–123.5	20.3–157.4	157.6–364.7	46.6–353.6
	OI	7.3 (0.8)	9.0 (1.2)	6.4 (1.2)	9.1 (1.0)	9.3 (2.2)	10.0 (1.3)	10.4 (1.5)	11.1 (2.2)
		6.4–8.2	7.1–10.9	5.2–8.9	7.9–10.4	6.1–12.6	8.2–12.4	8.6–12.7	6.1–13.8
	DTI	1.7 (0.3)	1.5 (0.4)	1.0 (0.2)	1.4 (0.4)	2.0 (1.2)	1.5 (0.5)	1.4 (0.3)	1.0 (0.2)
		1.3–2.2	0.6–2.1	0.7–1.4	0.9–1.9	0.9–4.6	0.9–2.5	1.1–2.0	0.9–1.4
Spawning potential	GSI	1.7 (0.3)	1.7 (0.2)	2.0 (0.2)	1.8 (0.2)	1.5 (0.3)	1.9 (0.2)	1.7 (0.1)	1.9 (0.2)
		1.4–2.1	1.4–2.0	1.6–2.4	1.6–2.0	1.1–2.1	1.7–2.2	1.4–1.9	1.4–2.1
	LIPIDS	26.2 (4.0)	17.8 (2.6)	20.3 (2.6)	25.2 (4.3)	18.1 (5.8)	16.3 (1.5)	16.6 (2.8)	16.5 (3.2)
		20.2–31.8	13.3–21.7	16.7–24.6	19.0–31.1	12.5–28.6	14.0–19.3	11.1–21.0	12.5–22.4
	RP	321.5 (78.1)	84.0 (28.4)	145.9 (103.3)	148.2 (85.4)	100.3 (59.3)	70.8 (35.0)	127.5 (129.7)	119.3 (83.9)
		241.0–490.1	48.0–122.4	29.1–400.2	60.7–338.1	55.2–234.8	31.6–151.7	26.9–445.9	36.9–257.6

The data for each life history trait show the mean (μ) ± standard deviation, and the minimum and maximum (min–max). The numbers of eels per catchment (*n*) sampled for the P11KT analysis are shown in brackets. TL: total length at silvering (mm), TW: total weight (g), GR: growth rate (mm·year^{-1}), AGE: estimated age (year), K: Fulton condition index (no unit), P11KT: plasma 11-ketotestoterone (pg·mL^{-1}), OI: Pankhurst's ocular index (%), DTI: digestive tract index (%), GSI: gonado-somatic index (%), LIPIDS: muscular lipid content (%), RP: reproductive potential index (g of eggs). Empty cells correspond to non-significant predictors.

We estimated the age with a sagittal otolith. Otoliths were cleaned, held in a longitudinal plane (Crystal Bond 509^{TM} thermal glue), embedded in epoxy resin (Araldite ®2020, Hunstman), sanded longitudinally from the dorsal face, and observed by four independent observers with a binocular microscope to count the continental growth annuli [45]. The GR represents the ratio between the growth in size during the continental phase (in mm) [46] and the continental age: GR = (TL − 65)/AGE. The K Fulton's body condition factor is computed as TW/TL^3 × 10^5 ratio [47]. The P11KT concentration was measured in plasma with the 11-KT Elisa Kit (Cayman Chemical Company, Ann Arbor, MI, USA) [48]. The Pankhurst's ocular index [35] is given by OI = [((A + B/4)^2 × π)/TL] × 100 with A and B the horizontal and vertical eyes diameters (mm), respectively. The digestive tract index is given by DTI = IWDFT/TW × 100 (with IWDFT the individual weight in g of full digestive tract) [37] and the gonado-somatic index is given by GSI = GW/TW × 100 (with GW the gonad weight in g) [37]. The reproductive potential index [49] is the potential mass of

egg produced by an eel: RP = [(TW × LIPIDS /100) − (TW × 0.0000145 × DSS)] × 1.72. The DSS is the distance in km from the sampling site to the spawning area estimated with 2.14.20 QGIS software [50]. The virtual migration corridor starts between the sampling site and the Azores inspired from previous studies [51] and continues to an average point of 27° N latitude and 55° W longitude (as the center of a 22–32° N latitude and 50–60° W longitude square; [52]).

LHTs were separated into four groups. Group 1 represents fecundity traits and includes the TL and TW both of which are positively correlated with the oocyte number [40,44]. Group 2 reflects the adaptability and plasticity abilities towards environmental heterogeneity, habitat types, carrying capacities and inter-intraspecific competitions, including the growth rate, the residence time and the body condition [42,43,53,54]. Group 3 represents the downstream migration readiness (P11KT, OI and DTI). The androgen 11-ketotestosterone is involved in triggering downstream migration and in the silvering process, during which OI and the degeneration of digestive tract increase [35,36,39,41]. Group 4 refers to the spawning potential, which depends in part on the maturation and silvering progress (GSI), muscular lipid reserves and the reproductive potential index.

2.6. Statistics

All coding, analysis and graphic representations were conducted in R software v. 4.0.2 under the tidyverse v. 1.3.0 environment [55,56].

2.7. Geographic Features

We selected four geographic predictors for each catchment: latitude and longitude of the sampling site (decimal degrees), salinity (freshwater and brackish water, classified by local expert statements) and catchment (drainage) area (km^2) from the European River and Catchment Database [57]. Eels were sampled in catchments with contamination and LHTs that were related to catchment identity. Thus, we implemented a factorial catchment effect (i.e., the ID of catchments, Table 1) as a local predictor in order to remove the effects of this catchment effect dependence.

2.8. Correlation between Predictors

We excluded all predictors with a Spearman correlation coefficient cutoff ± 0.7 {caret package, v. 6.0–86} [58]. The Spearman's correlation was important (coefficient ≥ 0.7) for seven of the 48 predictors: migration distance (DSS, correlated with longitude, r = 0.86), PBDEs (with HCB, r = 0.74), HBCDs (with HCB, r = 0.73), muscular Co (with Co in livers, r = 0.88), hepatic Hg (correlated with Hg in muscles, r = 0.87), gonadic Co (with Co in livers, r = 0.77) and gonadic Hg (with Hg in muscles, r = 0.86). After this step, the 41 predictors used in models included four geographic predictors, one catchment effect predictor, 35 predictors of chemical contamination (four groups of organic pollutants and 31 trace elements in different organs) and the *A. crassus* abundance.

2.9. Non-Parametric Models

For each LHT, we implemented one model with geographic predictors and a local (catchment) effect (GLP model) and second coupling geographic, contaminations (chemical and parasitism) and a local effect (GCP model). The GLP and GCP models were built with the no prior assumptions from a random forest RF algorithm {randomForest package, v. 4.6–14} [59] which is efficient for low-sample-size high-dimensional data [60]. The concept and step by step operation of the random forest RF are extensively described in previous articles [59,61,62].

For each *t* life history trait and *p* predictor, we computed a pseudo-R^2 as a partition of the total variance value by each predictor importance: pseudo $R^2 = (R_t{}^2 \times I_{tp})/\sum_{p'} I_{tp'}$, with $R_t{}^2$ the total variance (%) for a *t* life trait, I_{tp} the importance (as the increase of mean squared error of prediction) of a *p* predictor for the t life trait and $\sum_{p'} I_{tp'}$ the importance sum of all *p*′ predictors [63]. Negative values of pseudo-R^2 were replaced by zero values.

2.10. Model Tuning

The construction of random forest models requires a number of independent regression trees in the forest (ntree), a number of predictors randomly selected at each node among whole predictors (mtry) and a maximum number of nodes (tree complexity) (Supplementary Table S2). We optimized the mtry value with tuneRF function {randomForest package} [59] that builds a multitude of trained RF from different mtry values and identifies the RF with the lowest out-of-bag error estimate. For the ntree and maxnodes optimization, we used multiple tree construction loops (train function with "rf" method, {caret package} [58]) with a tree number between 250 and 2000, and a node number between 2 and 50 and we conserved the values that produced RF optimizing the pseudo-R^2.

2.11. Significance Tests

We used permutation tests to identify predictors that provided significant information in tree construction {rfPermute package, v. 2.1–81} [64]. These tests compare the distribution of importance scores between random forests with nrep permutations of a predictor observations (here, nrep = 500) and random forests without permutations.

2.12. Contribution Ratios

We computed the local (catchment) effect contribution compared to the geographic predictors in GLP models as the Ca/(Ca + G) × 100 ratio (noted Ca/G) between the pseudo-R^2 of the catchment effect (Ca) and those of the geographic predictors (G). Similarly, we computed in the GCP model the C/G ratio as the relative contribution of contaminants (C: sum of R^2 of significant contaminants) compared to the geographic predictors (G, without the catchment effect) and the TEs/POPs ratio as the relative contribution of trace elements compared to organic pollutants. For the contribution of gonadic trace elements (TE_gon) compared to all trace elements (TEs), we computed TE_gon/TEs × 100.

2.13. Trend Extraction

We extracted the trend of the marginal effect between a significant predictor and its associated LHT with the partial dependence plot (PDP, partialPlot function, {randomForest package} [59]) of the random forest's outputs. We performed an automatic trend extraction by applying a gaussian's generalized additive model (GAM, {mgcv package, v. 1.8–33} [65]). In each GAM, the partial dependant curve was cut in k partitions and a cubic regression spline was used to penalize the computed smooth coefficient at each k partition. Finally, we calculated the average of the k smoothed coefficients to automatically extract the positive or negative trends of PDP correlation for each predictor. A positive average coefficient indicated an averaged positive marginal effect of a significant predictor on the LHT response.

2.14. Contamination Scenarios

We designed two virtual and conceptual bioaccumulation scenarios from the observed contamination data (Supplementary Table S3). The optimistic scenario (low bioaccumulation) includes 100 virtual eels with randomly simulated contaminant values according to a uniform distribution between the minimum and maximum values of the observed quartile 0–25% (runif function, {stats package, v. 4.1.0} [56]). The pessimistic scenario (high bioaccumulation) is based on the 75–100% quartile. We assigned this virtual batch of 100 slightly or strongly contaminated eels to each studied catchment (i.e., 800 eels for the eight catchments and each scenario), taking care to preserve the observed values of the geographic predictors. The *A. crassus* abundance simulations were performed between the minimum and maximum values of all observed data for each catchment.

2.15. Prediction of Phenotypic Reaction

We predicted LHTs for optimistic and pessimistic scenarios from observed data (GCP models) using the rfinterval package (v. 1.0.0) that produces a 95% confidence interval of

prediction based on the empirical distribution of OOB observations [66,67]. We averaged the prediction of each trait and scenarios in order to measure the average phenotypic reaction (ω_t) throughout an increasing gradient of bioaccumulation as the proportional difference (in %) from optimistic to pessimistic scenarios: $\omega_t = (\hat{t}_{pessimistic} - \hat{t}_{optimistic} / \hat{t}_{pessimistic} + \hat{t}_{optimistic}) \times 100$, with $\hat{t}$ the predicted average of the t life trait under pessimistic or optimistic virtual conditions. Similarly, we calculated the proportional difference between the observed situation and the optimistic scenario [$\omega_t = (\hat{t}_{optimistic} - \hat{t}_{observed} / \hat{t}_{optimistic} + \hat{t}_{observed}) \times 100$], and the observed situation and the pessimistic scenario [$\omega_t = (\hat{t}_{observed} - \hat{t}_{pessimistic} / \hat{t}_{observed} + \hat{t}_{pessimistic}) \times 100$]. We compared the mean of traits between each condition (optimistic, pessimistic and observed) with two-sided Dunn's tests (Bonferroni correction, α = 5%, {FSA package, v. 0.8.30} [68]) because the normality of residues and homoscedasticity were not maintained.

We estimated the mean absolute fecundity in the optimistic, observed and pessimistic conditions from the back-calculated estimation of four regression equations between the TL (mm) and the number of oocytes per European eel (in millions):

$$\left(10^{-2.992+3.293 \times \log 10\ (\hat{TL})}\right) / 10^6 \quad (1)$$

$$\left(10^{-1.541+2.834 \times \log 10\ (\hat{TL})}\right) / 10^6 \quad (2)$$

$$\left(10^{-2.772+3.254 \times \log 10\ (\hat{TL})}\right) / 10^6 \quad (3)$$

$$\left(17,614 \times \hat{TL} - 10^7\right) / 10^6 \quad (4)$$

with $\hat{TL}$ the predicted or observed values of the total length [40,44,69,70].

3. Results

In the model using just 'GLp', the overall explained variance in LHTs was relatively low (42.4% to 9.3%, Figure 2a) and the local effect was usually the strongest predictor of variance, contributing between 23% to 99.5% (Table 3). The remaining GLP predictors alone explained a relatively low proportion of the significant variance (0.2% to 29.7%). This was inconsistent with previous studies suggesting that length, growth rate and age of silver eels are all strongly related to latitude, temperature and primary productivity [7,71–73]. In our analysis, the strongest relationships between GLP (including the local effect) and LHTs were obtained for lipids (42.4%—although this falls to 29.7% if the local effect is ignored) and the RP (35.3%–26% without local effect), together with two migratory readiness traits, 11-ketotestosterone (37.2%–0.2% without local effect) and ocular index (39.6%–26% without local effect) (Table 3). The GLP models explained a smaller proportion of the variance of adaptability traits, with 23.1% for age (17.9% without local effect), 24.8% for the growth rate (17.8% without local effect), and 30% for body condition (13.6% without local effect). Finally, the maturity indices (DTI and GSI) and fecundity traits (TL and TW) were predicted most poorly, with explained variance ranging between 9.3% and 18.3%. Although the relationships were weaker than expected [7], latitude and longitude positively correlated with almost all LHTs (Figure 3). Eels in northern and eastern Europe were older, larger, fatter and with greater reproductive potential than eels from the south and west of Europe. Exceptions to this general trend were growth rate (negative correlation with latitude), physical condition and GSI (negative correlations with longitude) and non-significant relationships for GSI (with latitude and salinity) and 11-ketotestosterone (with latitude and longitude). Catchment area explained 1.2% to 6% of variances and was not significant for weight and 11-ketotestosterone. Salinity had a negative but weak correlation with most LHTs, accounting for 0.2% to 5.5% of the variance, excepting for DTI and age (positive correlations). Overall, the results suggest that LHTs variation is influenced most strongly by local factors, i.e., those intrinsic to each catchment, with geographic factors having a significant but weak influence.

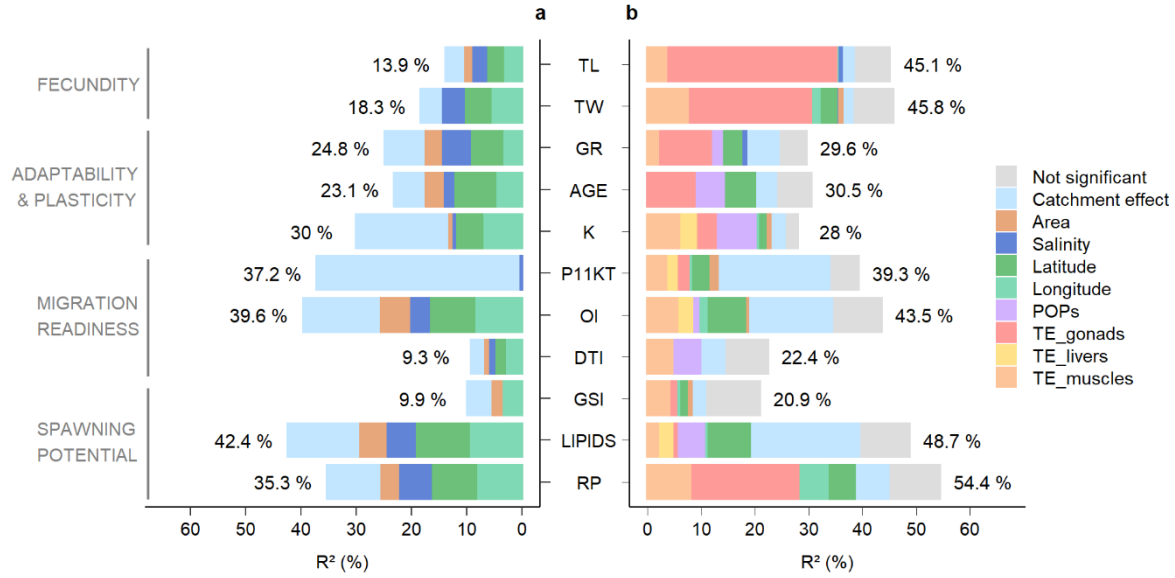

Figure 2. The explanatory power of environmental factors on the life history traits of 75 female silver eels. Stacked bars show how much each factor contributed to explaining the total and partial pseudo-variances (R^2, %) of each life history trait using a model with (**a**) geographic and local predictors [GLP models including catchment area, salinity, latitude, longitude and catchment (local) effect] and (**b**) contamination, geographic and local predictors [GCP models with additional contamination predictors: muscular POPs (persistent organic pollutants) and gonadic, hepatic and muscular TEs (trace elements)].

Table 3. Geographic and local models outputs. Related to Figures 2 and 3.

		Geographic Predictors (G)					Ca	Ratio (%)
Traits	**Total**	**Area**	**Lat**	**Long**	**Sal**	**Total G**		**Ca/G**
TL	13.9	1.9 (↗)	3.5 (↗)	3.0 (↗)	2.3 (↘)	10.7	3.2	23.0
TW	18.3		5.3 (↗)	5.3 (↗)	3.7 (↘)	14.3	4.0	21.9
GR	24.8	3.5 (↘)	6.3 (↘)	3.2 (↗)	4.8 (↘)	17.9	7.0	28.1
AGE	23.1	4.0 (↗)	8.1 (↗)	4.4 (↗)	1.4 (↗)	17.9	5.2	22.5
K	30.0	1.2 (↘)	5.4 (↗)	6.7 (↘)	0.3 (↘)	13.6	16.4	54.7
P11KT	37.2				0.2 (↘)	0.2	36.9	99.5
OI	39.6	6.0 (↘)	8.7 (↗)	8.2 (↗)	3.2 (↘)	26	13.6	34.3
DTI	9.3	1.4 (↗)	2.3 (↗)	2.7 (↗)	0.7 (↗)	7.1	2.2	23.7
GSI	9.9	2.5 (↘)		3.3 (↘)		5.8	4.1	41.4
LIPIDS	42.4	5.4 (↗)	10.2 (↗)	9.3 (↗)	4.7 (↘)	29.7	12.7	30.0
RP	35.3	3.8 (↗)	8.6 (↗)	7.9 (↗)	5.5 (↘)	25.8	9.5	26.9

Pseudo-variance (R^2, %) of significant geographic and local predictors (GLP) that explain the variation in the fitness-related traits of female silver eels. Empty cells correspond to non-significant predictors and arrows in parentheses indicate the correlation trends between significant GLP and traits. The Ca/G ratio measures the relative importance of the local (catchment) effect (Ca) compared to the geographic and environmental predictors (G). Lat: latitude; Long: longitude; Sal: salinity; Total G: Area + Lat + Long + Sal; Ca: catchment effect. All models have 75 eels except P11KT (n = 62).

The inclusion of contamination predictors, which are suspected to reduce the fitness of eels [18,20–26], improved the explanatory power of the models (hereafter 'GCp') for most LHTs, and reduced the proportion of the variance explained by 'GLp' (Figure 2b). The four best fits were obtained for traits related to fecundity (TW: 45.8%, a difference of 27.5%

with the GLP model; and TL: 45.1%, up by 31.2%) and those related to migratory readiness (RP index: 54.4%, up by 19.1%; and lipid content: 48.7%, up by 6.3%). Surprisingly, *A. crassus* infection did not have significant explanatory power for LHTs (included in the non-significant proportion of variance in Figure 2b), even though the infection is known to affect eel physiology [19]. In contrast to GLP models, the proportion of variability explained by the local effect in GCP models was generally much lower, indicating that contaminants had a significant impact on LHTs relative to geographical predictors. The proportion of variability associated with contaminants in GCP models exceeded 70% for seven of 11 traits (ratio C/G, Table 4), particularly for TL (97.1%) and DTI (100%). However, the local effect remained high for 11-ketotestosterone (21.3%), and was slightly increased for lipid contents (+8.1%) and ocular index (+2.5%) compared to GLP models. Of the contaminants, trace elements explained more variance in LHTs compared to organic pollutants (DDTs, HCB and PCBs), and in some cases explained 100% of variance (TL, TW, PIIKT, GSI and RP) (Table 4). The effect of trace elements was particularly strong in gonadal tissue, accounting for >70% of variation in the TL, TW, growth rate, age and RP index (ratio TE_gon/TEs, Table 4).

Table 4. | Geographic, local and contamination models outputs. Related to Figures 2 and 6.

		Geographic Predictors (G)					Ca	Contamination Predictors (C)								Ratio (%)			
								Trace Elements				Persistent Organic Pollutants				Total C	C/G	TEs/POPs	TE_Gon/TEs
Traits	Total	Area	Lat	Long	Sal	Total		TE_Gon	TE_Liv	TE_Musc	Total	DDTs	HCB	PCBs	Total				
TL	39			0.7 (↗)	0.3 (↘)	1.0	2.6	32.0		3.5	35.0					35.0	97	100	90
TW	39	0.6 (↗)	2.7 (↗)	2.1 (↗)	0.6 (↘)	5.9	2.3	23.0		7.5	30.0					30.0	84	100	75
GR	25		3.6 (↘)		0.9 (↘)	4.5	6.4	10.0		1.9	12.0		1.7		1.7	14.0	76	88	84
AGE	24		5.8 (↗)			5.8	4.5	9.3			9.3.0		4.9		4.9	14.0	71	65	100
K	26	0.9 (↘)	0.9 (↗)	0.9 (↗)		2.7	3.1	4.1	2.7	6.4	13.0	1.1	1.3	4.4	6.9	20.0	88	66	31
P11KT	34	1.8 (↗)	2.7 (↘)	1.0 (↘)		5.5	21	2.1	1.5	4.0	7.6					7.6	58	100	28
OI	35	0.6 (↘)	6.7 (↘)	2.0 (↘)		9.3	16		2.3	6.0	8.3			1.2	1.2	9.5	51	88	0
DTI	15					0	5.0			5.0	5.0		1.3	3.5	4.8	9.8	100	51	0
GSI	11	0.9 (↘)	1.0 (↘)	1.0 (↘)		3.0	3.0	1.3		4.0	5.3					5.3	64	100	25
LIPIDS	40		7.6 (↗)	0.9 (↗)		8.5	21	1.3	2.1	2.5	5.9		4.6		4.6	11.0	55	56	22
RP	45		4.6 (↗)	5.9 (↗)		11.0	6.7	20.0		7.9	28.0					28.0	73	100	72

Model performance is expressed as pseudo-variance (R^2, %) scores that explain the variation in the fitness-related traits of female silver eels given for significant geographic (G; Lat: latitude; Long: longitude; Sal: salinity), local (catchment effect Ca) and contamination (C) predictors. Different ratios were calculated: C/G (relative importance of the contaminants compared to the geographic predictors), TEs/POPs (trace elements (TEs) compared to muscular persistent organic pollutants (POPs)) and TE_gon/TEs (gonadic TEs compared to all TEs). The total variance represents the variance for all significant predictors, G predictors, TEs and POPs predictors and all C predictors. Empty cells correspond to non-significant predictors and arrows in parentheses indicate the correlation trends between significant G predictors and traits. All models have 75 eels except P11KT (n = 62).

In general, the GCP models showed negative trends between trace elements and fecundity (TL and TW), adaptability (K) and reproductive success traits (lipid content and RP) (Figure 3). For these traits, the trends of individual contaminants were usually in the opposite direction to those of geographic and local factors (except salinity). Overall, Ni and Mn concentrations in gonads explained a large variance for TL (23.8%), TW (17%) and RP index (12.7%), whereas Mn in livers and gonads influenced lipid content (2.1% and 1.3% respectively). Se explained some of the variability of the TL (gonads: 3.1%, muscles: 3.5%), TW (gonads: 1.7%, muscles: 6.4%), RP (muscles: 8%) and lipid content (muscles: 2.5%). Cr and Zn also influenced these traits (Figure 6 and Supplementary Figure S1). Body condition (K) was negatively influenced by contaminants in muscles

(Cd, HCB, DDT and PCBs), gonads (Cd, Cr and Zn) and livers (Cd and Pb). However, several contaminants were positively correlated with some LHTs (Figure 6). For example, although HCB and gonadic Cd negatively influenced growth rate, they were positively related to age. Muscular and gonadic As concentrations were positively related to growth rate. Overall, contaminants were positively related to silvering processes and migration readiness: various contaminants in muscles (As, Cd, HCB, Hg, Pb, PCBs and Se) and livers (Mn and Fe) influenced positively 11-ketotestosterone, OI, DTI and GSI traits. These results underline the ecotoxicity of trace elements, such as Ni or Se [74], and POPs which negatively influenced a number of important LHTs.

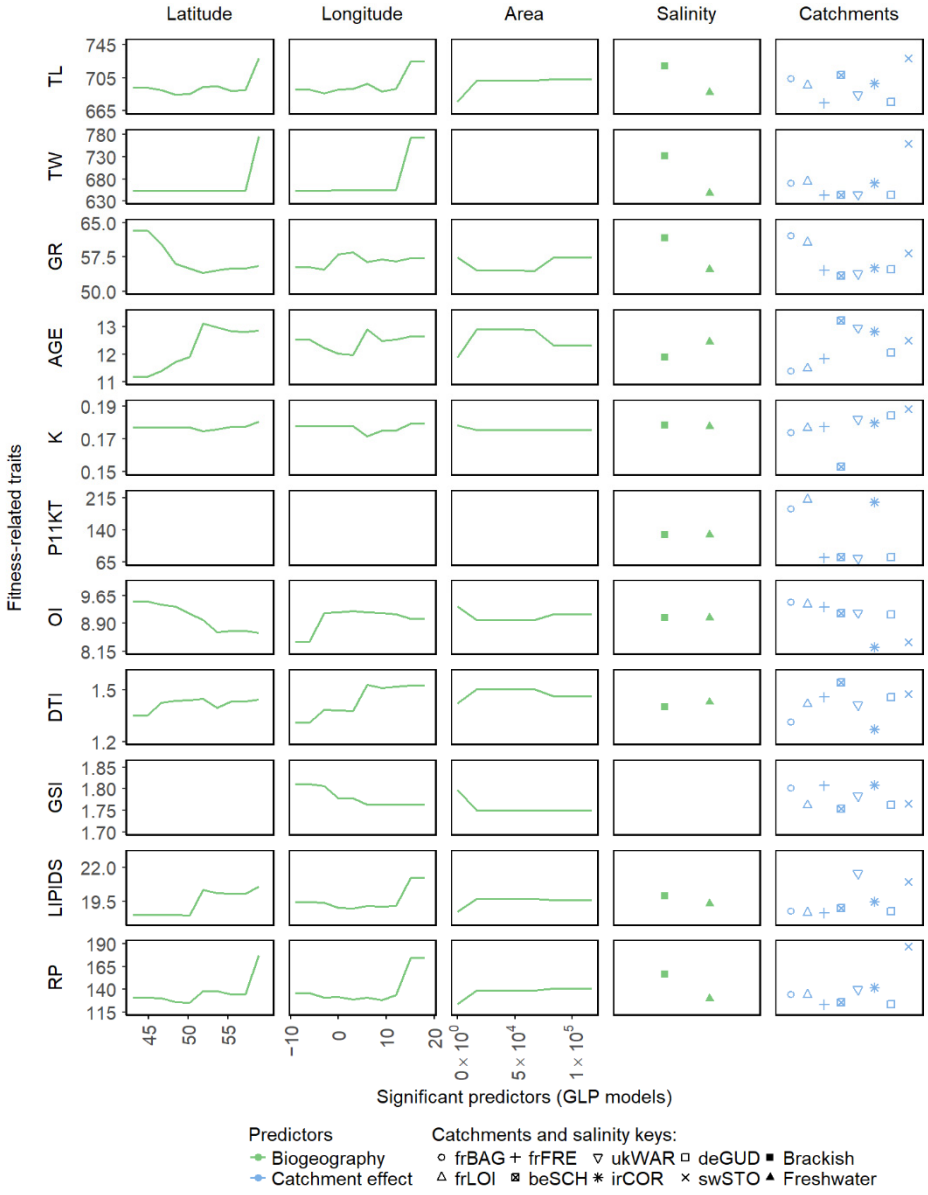

Figure 3. Marginal effect of geographic and local predictors (GLP models) on silver eel traits. Related to Figure 6. Plots show the partial dependence of significant GLP predictors after permutation test (n = 75 silver eels, 62 for P11KT trait). TL: total length at silvering (mm), TW: total weight (g), GR: growth rate (mm·year^{-1}), AGE: estimated age (year), K: Fulton condition index (%), P11KT: plasma 11-ketotestoterone (pg·mL^{-1}), OI: Pankhurst's ocular index (no unit), DTI: digestive tract index (%), GSI: gonado-somatic index (%), LIPIDS: muscular lipid content (%), RP: reproductive potential index (g of eggs). Empty cells correspond to non-significant predictors.

To assess the cumulative impact of contaminants on the expression of LHTs and eel reproductive potential, we compared the mean phenotypic reaction (ω) under pristine and pessimistic contamination scenarios (i.e., at the lower and upper end of the contamination levels observed in our samples; see methods section). The contamination is divided by five between observed and optimistic situations, and multiplied by four between observed and pessimistic situations, resulting in an average level of 29 times between the pessimistic and the optimistic scenarios (see Supplementary Table S3).

The results show that female silver eels in heavily contaminated catchments would be significantly smaller ($\omega_{TL} = -15.9\%$, $z = -35.0$, $p = 2.1 \times 10^{-268}$), lighter ($\omega_{TW} = -40.0\%$, $z = -34.4$, $p = 7.0 \times 10^{-259}$) with a reduced body condition ($\omega_K = +15.6\%$, $z = -35.3$, $p = 1.8 \times 10^{-272}$) compared to eels from pristine catchments (Figure 4, Supplementary Figure S2). Interestingly, compared to the initial situation, the age increased more under a highly degraded scenario than under an improved scenario, and might be a consequence. Conversely, all the other LHT showed contrasted responses to the scenarios with a decrease (6 LHT) or an increase (3 LHT) under the pessimistic and an opposite either increase (6 LHT) or decrease (3 LHT) under the optimistic scenario. The integration of these impacts is a direct effect on individual fecundity, equivalent to a reduction of 3.1 times compared to the pristine situation ($\omega_{fecundity} = -51.3\%$, $z = -105.2$, $p < 0.05$) (Figure 5). Between observed LHTs and pessimistic scenario, the negative effect of contamination was low ($\omega_{TL} = -6.1\%$, $\omega_{TW} = -9.9\%$, $\omega_{GR} = -0.6\%$, $\omega_K = -10.2\%$, $\omega_{LIPIDS} = -1.8\%$ and $\omega_{RP} = -7.9\%$) (Figure 4), but the combined effect on LHTs had a 1.8 times reduction in fecundity (Figure 5). This suggests that low levels of contamination can have a significant effect on reproductive potential and that remediation of contamination may be a viable management option for increasing the resilience of eel populations. For example, the current recruitment of glass eels in Europe (ca. 440 tons, [75]) would reach 792 tons if contamination could be reduced to low levels. This increase represents 6.2 times the annual mean glass eel catches range between 2013 and 2017 in Europe (56.5 tons) [27]. The reduction and remediation of pollution may therefore be an efficient, but currently underestimated, way to improve the reproductive potential and the resilience of this critically endangered species.

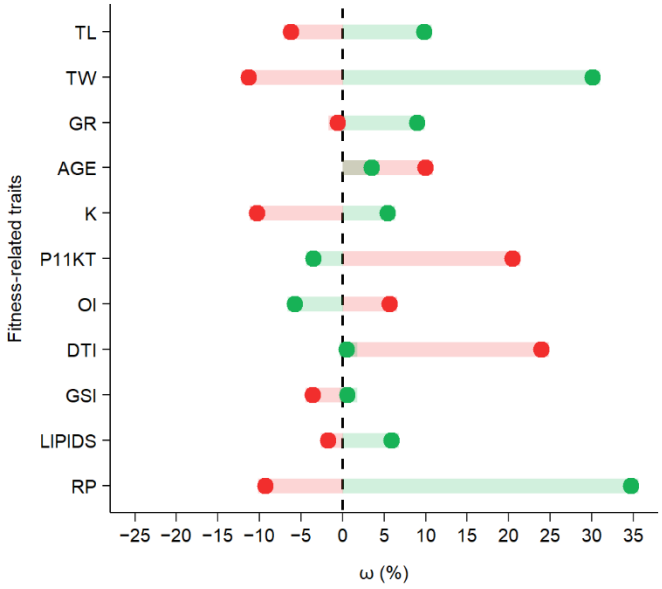

Figure 4. Average phenotypic reaction of female silver eel traits along a simulated gradient of contamination. The phenotypic reaction (ω) was computed as the proportional variation between the average of observed life history traits (centred and dashed line) and the average of predicted traits in the optimistic (low bioaccumulation) or pessimistic (high bioaccumulation) scenarios.

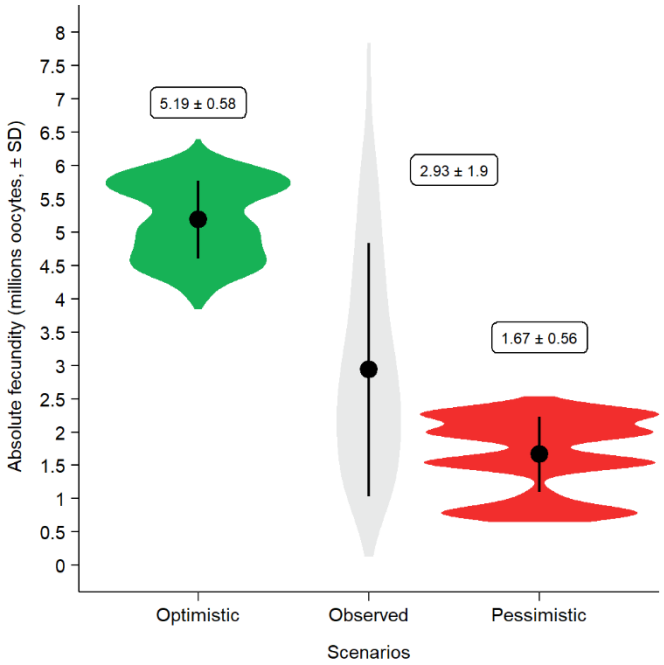

Figure 5. Impact of an increasing bioaccumulation gradient on European eel fecundity. Violin plot and averages (black dots, ± standard deviation SD) of the absolute fecundity (million oocytes per eel) estimated from the length of sampled eels and simulated eels in optimistic (low bioaccumulation) and pessimistic (high bioaccumulation) scenarios according GCP models (geographic, local and contamination predictors).

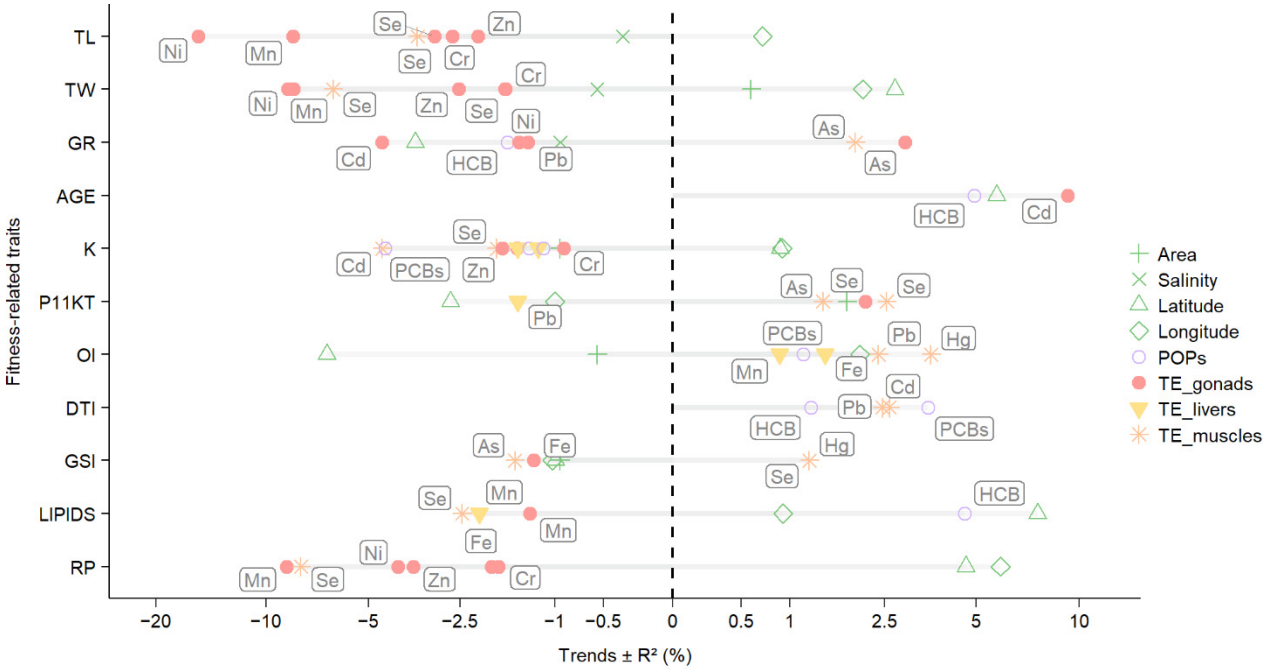

Figure 6. Trends between life history traits of 75 female silver eels and the geographic and contaminants predictors (GCP models). The significant predictors (POPs: persistent organic pollutants, TEs: trace elements) were distributed throughout their explained pseudo-variance gradients (R^2, %), that signs were assigned by tendencies of the marginal effect of each predictor on traits. The name of the significant contaminant predictor is displayed at each point. The local (catchment) effect was not reported.

4. Discussion

Overall, our results suggest that the effect of contamination by trace elements and organic pollutants significantly over-rides the biogeographical impacts of LHTs across our sampling from the European eel's area distribution, and undermines the phenotypic response of eels to their environment. We propose this impact is the consequence of the displacement of energy from growth and physiological processes to detoxification [20,23,76]. The excretion of excess trace elements would reduce growth rate, lipid storage and reducing reproductive investment between optimistic and pessimistic scenarios (ω_{GR} = −9.6 %, z = −31.3, $p = 4.2 \times 10^{-215}$; ω_{LIPIDS} = −7.7%, z = −23.0, $p = 7.0 \times 10^{-117}$ and ω_{RP} = −42.7%, z = 34.1, $p = 6.6 \times 10^{-255}$). The eels would presumably compensate for this fitness deficit by residing longer in catchments (+1.8 years, ω_{AGE} = +6.6%, z = 30.5, $p = 1.4 \times 10^{-203}$). Consequently, eels will be more exposed to lipophilic contaminants such as POPs and some trace elements (As, Hg, Pb and Cd) (Figure 2). These contaminants appear likely to lead to precocious downstream migration before physiological thresholds are met. High levels of contamination are linked to an increase of 11-ketotestosterone concentration and ocular and digestive tract indices that indicate readiness to migrate (ω_{P11KT} = +23.8%, z = 33.7, $p = 5.4 \times 10^{-248}$; ω_{OI} = +11.4%, z = 34.2, $p = 4.5 \times 10^{-256}$ and ω_{DTI} = +23.8%, z = 34.1, $p = 1.0 \times 10^{-254}$). The impacts of contaminants likely continue into the reproductive phase because eels also appear to mitigate toxic effects by transferring contaminants to gonad tissue [31,32,77]. Whilst partitioning contamination to a non-somatic tissue reduces immediate impacts, effects on life-time fitness may be very significant when coupled with effects on growth and fat content, with for example a direct reduction on maturation (ω_{GSI} = −4.1%, z = −33.8, $p = 1.5 \times 10^{-249}$). Furthermore, during the transoceanic migration of fasting eels, released contaminants likely provoke secondary toxicity [18,24,77,78] and contaminants can be transferred to the developing eggs [31,32], which might hinder egg and embryo survival [21]. The cumulative impact of contamination therefore seems to hamper, at an individual level, egg production and the likelihood of migration to the remote spawning areas [38,79]. This strongly supports the idea that overfishing is not the only dominant cause of the eel's decline. Adverse sublethal impacts of pollutants have been described on many marine species' physiology, reproductive success, survival and population dynamics [80–83].

In conclusion, our study demonstrates an innovative approach to quantify the effects of contamination on European eel life history traits, an indicator of the global biodiversity crisis [15]. Although further validation is necessary, using a more extensive sample that would include a wider range of environmental situations, our results provide evidence that contaminants in sampled female silver eels skew the expression of traits and reduce the phenotypic resilience of individuals to environmental variability [84], which in turn could have potential effects at the population level. We speculate that contamination of animals by anthropogenic compounds is probably a fundamental contributor to biodiversity loss. Understanding the effects of pollution on phenotypic responses could help conservation strategies to limit biodiversity loss and to reduce the cumulative pressures on endangered species. Acting on the contamination is undoubtly a major conservation issue, that would have a highly significant political, sociological and economic cost. However, how much this is an option is a crucial question for the future, in the frame of the necessary ecological transition.

Supplementary Materials: The following supporting information can be downloaded at: https://www.mdpi.com/article/10.3390/fishes7050274/s1, Table S1: Chemical contaminant concentrations and *A. crassus* abundance measured in the female silver eels sampled from each European catchment; Table S2: Settings and total pseudo-variance outputs of GLP and GCP random forest models; Table S3: Design of bioaccumulation scenarios; Figure S1: The marginal effect of geographic, local and contamination predictors (GCP) on the female silver eel fitness-related traits; Figure S2: Distribution of fitness-related traits of female silver eels across an increasing bioaccumulation gradient.

Author Contributions: B.B. and E.F. contributed equally to this work. D.R. administered and coordinated the EELIAD project, while E.F. coordinated the eel quality work-package; B.B and E.F. developed the initial concept; D.R., E.F. and A.A. designed the sampling protocol; A.A. managed and centralized samples between collaborators; B.B. pooled results and analyzed models with T.T. and N.T contributions; S.D. measured the 11-ketotestosterone concentration; B.B., E.F. and D.R. developed theory and co-wrote the manuscript. B.B, E.F., A.A., T.T., N.T., C.B., P.B., S.D., K.A., A.W. and D.R. substantially participated in the revision of the intellectual content of the manuscript. All authors have read and agreed to the published version of the manuscript.

Funding: This research was funded by the European Union FP7 research program on Environment which supported the EELIAD program (EU-EELIAD 2008-2012, grant number GOCE-2008212133).

Institutional Review Board Statement: Ethical review and approval for this study was performed according to the ethical standards before 2008 of each participating institute.

Data Availability Statement: The contaminants and life history traits data that support the findings of this study are available from the corresponding author upon reasonable request.

Acknowledgments: We thank the European Union FP7 research program on Environment, which supported the EELIAD program. We thank all the professional fishermen and scientific institutes who contributed to the large sampling, particularly Håkan Wickström and Niklas Sjöberg (Swedish University of Agricultural Sciences), Michael Ingemann Pedersen (Technical University of Denmark), Michael Godard (Cefas, England), Liz Baldwin (Environment Agency, England), Russell Poole (Ireland Marine Institute), Paddy Gargan and Gustavo Becerra-Jurado (Inland Fisheries Ireland), Gregory E. Maes (KU Leuven, Belgium), Clarisse Boulenger (Agrocampus of Rennes, France), Catherine Boisneau (University of Tours, France) and Javier Lobón-Cerviá (Madrid National Museum of Natural Science, Spain). We appreciate the participation of Romain Gadais, Raymonde Lecomte-Finiger, Simon Pottier, and Gael Simon for the eel dissections. We appreciate the collaboration during the EELIAD program with Adrian Covaci and Govindan Malarvannan from the Toxicological Center (University of Antwerp, Belgium) for the persistent organic pollutants and lipids measurements, Carine Churlaud and Nicolas Delage from the LIENSs laboratory (University of La Rochelle, France) and Lieven Bervoets from the Antwerp University (Belgium) for the trace elements analysis, Elisabeth Faliex and Elsa Amilhat from CEFREM center (Perpignan University, France) for the parasite diagnostics, Laure-Sarah Virág and Élodie Réveillac from CRESCO center (National Museum of Natural History, Dinard, France) for age estimation, and the BOREA laboratory (National Museum of Natural History, Paris, France) for hormones analysis. The IUF (Institut Universitaire de France) is acknowledged for its support to PB as a senior member.

Conflicts of Interest: The authors declare no conflict of interest.

References

1. Aoyama, J.; Nishida, M.; Tsukamoto, K. Molecular Phylogeny and Evolution of the Freshwater Eel, Genus *Anguilla*. *Mol. Phylogenet. Evol.* **2001**, *20*, 450–459. [CrossRef] [PubMed]
2. Barth, J.M.I.; Gubili, C.; Matschiner, M.; Tørresen, O.K.; Watanabe, S.; Egger, B.; Han, Y.S.; Feunteun, E.; Sommaruga, R.; Jehle, R.; et al. Stable Species Boundaries despite Ten Million Years of Hybridization in Tropical Eels. *Nat. Commun.* **2020**, *11*, 1–13. [CrossRef]
3. Tsukamoto, K.; Kuroki, M.; Watanabe, S. Common Names for All Species and Subspecies of the Genus *Anguilla*. *Environ. Biol. Fishes* **2020**, *103*, 985–991. [CrossRef]
4. Miller, M.J.; Bonhommeau, S.; Munk, P.; Castonguay, M.; Hanel, R.; McCleave, J.D. A Century of Research on the Larval Distributions of the Atlantic Eels: A Re-Examination of the Data. *Biol. Rev.* **2015**, *90*, 1035–1064. [CrossRef] [PubMed]
5. Tesch, F.W. *The Eel*, 3rd ed.; Thorpe, J.E., Ed.; Wiley-Blackwell: Oxford, UK, 2003; ISBN1 9780632063895. ISBN2 9780470995389.
6. Larsson, P.; Hamrin, S.; Okla, L. Fat Content as a Factor Inducing Migratory Behavior in the Eel (*Anguilla anguilla* L.) to the Sargasso Sea. *Naturwissenschaften* **1990**, *77*, 488–490. [CrossRef]
7. Vøllestad, L.A. Geographic Variation in Age and Length at Metamorphosis of Maturing European Eel: Environmental Effects and Phenotypic Plasticity. *J. Anim. Ecol.* **1992**, *61*, 41–48. [CrossRef]
8. Svedäng, H.; Neuman, E.; Wickström, H. Maturation Patterns in Female European Eel: Age and Size at the Silver Eel Stage. *J. Fish Biol.* **1996**, *48*, 342–351. [CrossRef]
9. Yokouchi, K.; Daverat, F.; Miller, M.J.; Fukuda, N.; Sudo, R.; Tsukamoto, K.; Elie, P.; Poole, W.R. Growth Potential Can Affect Timing of Maturity in a Long-Lived Semelparous Fish. *Biol. Lett.* **2018**, *14*, 20180269. [CrossRef] [PubMed]

10. Drouineau, H.; Rigaud, C.; Daverat, F.; Lambert, P. EvEel (Evolutionary Ecology-Based Model for Eel): A Model to Explore the Role of Phenotypic Plasticity as an Adaptive Response of Three Temperate Eels to Spatially Structured Environments. *Can. J. Fish. Aquat. Sci.* **2014**, *71*, 1561–1571. [CrossRef]
11. Mateo, M.; Lambert, P.; Tetard, S.; Castonguay, M.; Ernande, B.; Drouineau, H. Cause or Consequence? Exploring the Role of Phenotypic Plasticity and Genetic Polymorphism in the Emergence of Phenotypic Spatial Patterns of the European Eel. *Can. J. Fish. Aquat. Sci.* **2017**, *74*, 987–999. [CrossRef]
12. Righton, D.; Piper, A.; Aarestrup, K.; Amilhat, E.; Belpaire, C.; Casselman, J.; Castonguay, M.; Díaz, E.; Dörner, H.; Faliex, E.; et al. Important Questions to Progress Science and Sustainable Management of Anguillid Eels. *Fish Fish.* **2021**, *22*, 762–788. [CrossRef]
13. Feunteun, E. Management and Restoration of European Eel Population (*Anguilla anguilla*): An Impossible Bargain. *Ecol. Eng.* **2002**, *18*, 575–591. [CrossRef]
14. Miller, M.J.; Feunteun, E.; Tsukamoto, K. Did a "Perfect Storm" of Oceanic Changes and Continental Anthropogenic Impacts Cause Northern Hemisphere Anguillid Recruitment Reductions? *ICES J. Mar. Sci.* **2016**, *73*, 43–56. [CrossRef]
15. Drouineau, H.; Durif, C.M.F.; Castonguay, M.; Mateo, M.; Rochard, E.; Verreault, G.; Yokouchi, K.; Lambert, P. Freshwater Eels: A Symbol of the Effects of Global Change. *Fish Fish.* **2018**, *19*, 903–930. [CrossRef]
16. Arevalo, E.; Lassalle, G.; Tétard, S.; Maire, A.; Sauquet, E.; Lambert, P.; Paumier, A.; Villeneuve, B.; Drouineau, H. An Innovative Bivariate Approach to Detect Joint Temporal Trends in Environmental Conditions: Application to Large French Rivers and Diadromous Fish. *Sci. Total Environ.* **2020**, *748*, 141260. [CrossRef] [PubMed]
17. Trancart, T.; Carpentier, A.; Acou, A.; Charrier, F.; Mazel, V.; Danet, V.; Feunteun, E. When "Safe" Dams Kill: Analyzing Combination of Impacts of Overflow Dams on the Migration of Silver Eels. *Ecol. Eng.* **2020**, *145*, 105741. [CrossRef]
18. Geeraerts, C.; Belpaire, C. The Effects of Contaminants in European Eel: A Review. *Ecotoxicology* **2009**, *19*, 239–266. [CrossRef]
19. Szekely, C.; Palstra, A.P.; Molnár, K.; van den Thillart, G.E.E.J.M. Impact of the Swimbladder Parasite on the Health and Performance of European Eels. In *Spawning Migration of the European Eel*; Springer: Berlin, Germany, 2009; Volume 30, pp. 201–226. [CrossRef]
20. Robinet, T.; Feunteun, E. Sublethal Effects of Exposure to Chemical Compounds: A Cause for the Decline in Atlantic Eels? *Ecotoxicology* **2002**, *11*, 265–277. [CrossRef]
21. Palstra, A.P.; van Ginneken, V.J.T.; Murk, A.J.; van den Thillart, G.E.E.J.M. Are Dioxin-like Contaminants Responsible for the Eel (*Anguilla anguilla*) Drama? *Naturwissenschaften* **2006**, *93*, 145–148. [CrossRef] [PubMed]
22. Pierron, F.; Baudrimont, M.; Gonzalez, P.; Bourdineaud, J.P.; Elie, P.; Massabuau, J.C. Common Pattern of Gene Expression in Response to Hypoxia or Cadmium in the Gills of the European Glass Eel (*Anguilla anguilla*). *Environ. Sci. Technol.* **2007**, *41*, 3005–3011. [CrossRef]
23. Pierron, F.; Baudrimont, M.; Bossy, A.; Bourdineaud, J.P.; Brèthes, D.; Elie, P.; Massabuau, J.C. Impairment of Lipid Storage by Cadmium in the European Eel (*Anguilla anguilla*). *Aquat. Toxicol.* **2007**, *81*, 304–311. [CrossRef] [PubMed]
24. Pierron, F.; Du Colombier, S.B.; Moffett, A.; Caron, A.; Peluhet, L.; Daffe, G.; Lambert, P.; Elie, P.; Labadie, P.; Budzinski, H.; et al. Abnormal Ovarian DNA Methylation Programming during Gonad Maturation in Wild Contaminated Fish. *Environ. Sci. Technol.* **2014**, *48*, 11688–11695. [CrossRef] [PubMed]
25. Oliveira, M.; Serafim, A.; Bebianno, M.J.; Pacheco, M.; Santos, M.A. European Eel (*Anguilla anguilla* L.) Metallothionein, Endocrine, Metabolic and Genotoxic Responses to Copper Exposure. *Ecotoxicol. Environ. Saf.* **2008**, *70*, 20–26. [CrossRef] [PubMed]
26. Maes, G.E.; Raeymaekers, J.A.M.; Hellemans, B.; Geeraerts, C.; Parmentier, K.; de Temmerman, L.; Volckaert, F.A.M.; Belpaire, C. Gene Transcription Reflects Poor Health Status of Resident European Eel Chronically Exposed to Environmental Pollutants. *Aquat. Toxicol.* **2013**, *126*, 242–255. [CrossRef]
27. ICES Joint EIFAAC/ICES/GFCM Working Group on Eels (WGEEL). *ICES Scientific Reports*; ICES: Copenhagen, Denmark, 2020; Volume 2. Available online: https://www.ices.dk/Community/Groups/Pages/WGEEL.Aspx (accessed on 15 June 2021).
28. Feunteun, E.; Prouzet, P. Forty Years of Decline and 10 Years of Management Plan: Are European Eels (*Anguilla anguilla*) Recovering. In *Evolution of Marine Coastal Ecosystems under the Pressure of Global Changes*; Springer International Publishing: Cham, Switzerland, 2020; pp. 269–295.
29. Belpaire, C.; Hodson, P.; Pierron, F.; Freese, M. Impact of Chemical Pollution on Atlantic Eels: Facts, Research Needs and Implications for Management. *Curr. Opin. Environ. Sci. Health* **2019**, *11*, 26–36. [CrossRef]
30. Durif, C.M.F.; Dufour, S.; Elie, P. Impact of Silvering Stage, Age, Body Size and Condition on Reproductive Potential of the European Eel. *Mar. Ecol. Prog. Ser.* **2006**, *327*, 171–181. [CrossRef]
31. Sühring, R.; Freese, M.; Schneider, M.; Schubert, S.; Pohlmann, J.D.; Alaee, M.; Wolschke, H.; Hanel, R.; Ebinghaus, R.; Marohn, L. Maternal Transfer of Emerging Brominated and Chlorinated Flame Retardants in European Eels. *Sci. Total Environ.* **2015**, *530–531*, 209–218. [CrossRef]
32. Freese, M.; Sühring, R.; Marohn, L.; Pohlmann, J.D.; Wolschke, H.; Byer, J.D.; Alaee, M.; Ebinghaus, R.; Hanel, R. Maternal Transfer of Dioxin-like Compounds in Artificially Matured European Eels. *Environ. Pollut.* **2017**, *227*, 348–356. [CrossRef]
33. Bourillon, B.; Acou, A.; Trancart, T.; Belpaire, C.; Covaci, A.; Bustamante, P.; Faliex, E.; Amilhat, E.; Malarvannan, G.; Virag, L.; et al. Assessment of the Quality of European Silver Eels and Tentative Approach to Trace the Origin of Contaminants—A European Overview. *Sci. Total Environ.* **2020**, *743*, 140675. [CrossRef] [PubMed]
34. CORDIS (Community Research Service). *Final Report Summary—EELIAD (European Eels in the Atlantic: Assessment of Their Decline)*; CORDIS: Luxembourg, Luxembourg, 2013.

35. Pankhurst, N.W. Relation of Visual Changes to the Onset of Sexual Maturation in the European Eel *Anguilla Anguilla* (L.). *J. Fish Biol.* **1982**, *21*, 127–140. [CrossRef]
36. Aroua, S.; Schmitz, M.; Baloche, S.; Vidal, B.; Rousseau, K.; Dufour, S. Endocrine Evidence That Silvering, a Secondary Metamorphosis in the Eel, Is a Pubertal Rather than a Metamorphic Event. *Neuroendocrinology* **2005**, *82*, 221–232. [CrossRef] [PubMed]
37. Durif, C.; Dufour, S.; Elie, P. The Silvering Process of *Anguilla Anguilla*: A New Classification from the Yellow Resident to the Silver Migrating Stage. *J. Fish Biol.* **2005**, *66*, 1025–1043. [CrossRef]
38. Belpaire, C.G.J.; Goemans, G.; Geeraerts, C.; Quataert, P.; Parmentier, K.; Hagel, P.; de Boer, J. Decreasing Eel Stocks: Survival of the Fattest? *Ecol. Freshw. Fish* **2009**, *18*, 197–214. [CrossRef]
39. Sudo, R.; Tosaka, R.; Ijiri, S.; Adachi, S.; Aoyama, J.; Tsukamoto, K. 11-Ketotestosterone Synchronously Induces Oocyte Development and Silvering-Related Changes in the Japanese Eel, *Anguilla Japonica*. *Zool. Sci.* **2012**, *29*, 254–259. [CrossRef] [PubMed]
40. MacNamara, R.; McCarthy, T.K. Size-Related Variation in Fecundity of European Eel (*Anguilla anguilla*). *ICES J. Mar. Sci.* **2012**, *69*, 1333–1337. [CrossRef]
41. Sudo, R.; Tsukamoto, K. Migratory Restlessness and the Role of Androgen for Increasing Behavioral Drive in the Spawning Migration of the Japanese Eel. *Sci. Rep.* **2015**, *5*, 1–7. [CrossRef] [PubMed]
42. Boulenger, C.; Acou, A.; Gimenez, O.; Charrier, F.; Tremblay, J.; Feunteun, E. Factors Determining Survival of European Eels in Two Unexploited Sub-Populations. *Freshw. Biol.* **2016**, *61*, 947–962. [CrossRef]
43. Geffroy, B.; Bardonnet, A. Sex Differentiation and Sex Determination in Eels: Consequences for Management. *Fish Fish.* **2016**, *17*, 375–398. [CrossRef]
44. MacNamara, R.; McCarthy, T.K.; Wickström, H.; Clevestam, P.D. Fecundity of Silver-Phase Eels (*Anguilla anguilla*) from Different Habitat Types and Geographic Locations. *ICES J. Mar. Sci.* **2016**, *73*, 135–141. [CrossRef]
45. *ICES Workshop on Age Reading of European and American Eel (WKAREA)*; ICES Scientific Reports; ICES: Copenhagen, Denmark, 2009.
46. Réveillac, É. *Histoires de Vie Larvaire et Dispersion Des Anguillidae: Vers Une Approche Bio-Évolutive*; University of La Rochelle: La Rochelle, France, 2008.
47. Fulton, T.W. The Rate of Growth of Fishes. *Fish. Board Scotl.* **1904**, *3*, 141–241.
48. Mazzeo, I.; Peñaranda, D.S.; Gallego, V.; Baloche, S.; Nourizadeh-Lillabadi, R.; Tveiten, H.; Dufour, S.; Asturiano, J.F.; Weltzien, F.A.; Pérez, L. Temperature Modulates the Progression of Vitellogenesis in the European Eel. *Aquaculture* **2014**, *434*, 38–47. [CrossRef]
49. ICES Report of the Joint EIFAAC/ICES Working Group on Eels (WGEEL). *ICES Scientific Reports*; ICES: Copenhagen, Denmark, 18–22 March 2013 in Sukarietta, Spain, 4–10 September 2013 in Copenhagen, Denmark; 2013. Available online: https://www.ices.dk/Community/Groups/Pages/WGEEL.aspx (accessed on 1 November 2020).
50. QGIS Development Team QGIS Geographic Information System. Open Source Geospatial Foundation Project. 2017. Available online: http://qgis.osgeo.org (accessed on 15 December 2017).
51. Righton, D.; Westerberg, H.; Feunteun, E.; Økland, F.; Gargan, P.; Amilhat, E.; Metcalfe, J.; Lobon-Cervia, J.; Sjöberg, N.; Simon, J.; et al. Empirical Observations of the Spawning Migration of European Eels: The Long and Dangerous Road to the Sargasso Sea. *Sci. Adv.* **2016**, *2*, e1501694. [CrossRef] [PubMed]
52. Friedland, K.D.; Miller, M.J.; Knights, B. Oceanic Changes in the Sargasso Sea and Declines in Recruitment of the European Eel. *ICES J. Mar. Sci.* **2007**, *64*, 519–530. [CrossRef]
53. Maes, G.E.; Raeymaekers, J.A.M.; Pampoulie, C.; Seynaeve, A.; Goemans, G.; Belpaire, C.; Volckaert, F.A.M. The Catadromous European Eel *Anguilla Anguilla* (L.) as a Model for Freshwater Evolutionary Ecotoxicology: Relationship between Heavy Metal Bioaccumulation, Condition and Genetic Variability. *Aquat. Toxicol.* **2005**, *73*, 99–114. [CrossRef] [PubMed]
54. Boulenger, C.; Crivelli, A.J.; Charrier, F.; Roussel, J.M.; Feunteun, E.; Acou, A. Difference in Factors Explaining Growth Rate Variability in European Eel Subpopulations: The Possible Role of Habitat Carrying Capacity. *Ecol. Freshw. Fish* **2016**, *25*, 281–294. [CrossRef]
55. Wickham, H. Easily Install and Load the "Tidyverse". 2019. Available online: https://tidyverse.tidyverse.org/ (accessed on 23 September 2019).
56. R Core Team. *R: A Language and Environment for Statistical Computing*; R Foundation for Statistical Computing: Vienna, Austria, 2020. Available online: https://www.r-project.org/ (accessed on 23 September 2020).
57. Vogt, J.; Soille, P.; de Jager, A.; Rimavičiūtė, E.; Mehl, W.; Foisneau, S.; Bódis, K.; Dusart, J.; Paracchini, M.L.; Haastrup, P.; et al. *A Pan-European River and Catchment Database, Version 2.0 (CCM2)*; European Commission: Luxembourg, 2007.
58. Kuhn, M.; Wing, J.; Weston, S.; Williams, A.; Keefer, C.; Engelhardt, A.; Cooper, T.; Mayer, Z.; Kenkel, B.; Benesty, M.; et al. *Package "caret"*; R Foundation for Statistical Computing: Vienna, Austria, 2020; pp. 1–224.
59. Liaw, A.; Wiener, M. Classification and Regression by RandomForest. *R News* **2002**, *2*, 18–22.
60. Biau, G.; Scornet, E. A Random Forest Guided Tour. *Test* **2016**, *25*, 197–227. [CrossRef]
61. Breiman, L.; Friedman, J.H.; Olshen, R.A.; Stone, C.J. *Classification and Regression Trees*, 1st ed.; CRC Press: Boca Raton, FL, USA, 1984; ISBN 9781351460491.
62. Breiman, L. Random Forests. *Mach. Learn.* **2001**, *45*, 5–32. [CrossRef]

63. Ellis, N.; Smith, S.J.; Pitcher, C.R. Gradient Forests: Calculating Importance Gradients on Physical Predictors. *Ecology* **2012**, *93*, 156–168. [CrossRef]
64. Archer, E. *RfPermute: Estimate Permutation p-Values for Random Forest Importance Metrics*; R Foundation for Statistical Computing: Vienna, Austria, 2020; pp. 1–22.
65. Wood, S. *Mixed GAM Computation Vehicle with Automatic Smoothness Estimation*; R Foundation for Statistical Computing: Vienna, Austria, 2020; pp. 1–322.
66. Zhang, H. *Predictive Inference for Random Forests (Rfinterval)*; R Foundation for Statistical Computing: Vienna, Austria, 2019; pp. 1–5.
67. Zhang, H.; Zimmerman, J.; Nettleton, D.; Nordman, D.J. Random Forest Prediction Intervals. *Am. Stat.* **2019**, *74*, 392–406. [CrossRef]
68. Ogle, D.; Wheeler, P.; Dinno, A. *FSA: Simple Fisheries Stock Assessment Methods*; R Foundation for Statistical Computing: Vienna, Austria, 2020; pp. 1–203.
69. Macnamara, R.; Koutrakis, E.T.; Sapounidis, A.; Lachouvaris, D.; Arapoglou, F.; Panora, D.; McCarthy, T.K. Reproductive Potential of Silver European Eels (*Anguilla anguilla*) Migrating from Vistonis Lake (Northern Aegean Sea, Greece). *Mediterr. Mar. Sci.* **2014**, *15*, 539–544. [CrossRef]
70. Dębowska, M.; Nowosad, J.; Targońska, K.; Żarski, D.; Biłas, M.; Łuczyńska, J.; Kucharczyk, D. Fecundity of Migrating European Eel (*Anguilla anguilla*) from Polish Waters. *Ital. J. Anim. Sci.* **2015**, *14*, 566–570. [CrossRef]
71. Oliveira, K. Life History Characteristics and Strategies of the American Eel, *Anguilla Rostrata*. *Can. J. Fish. Aquat. Sci.* **1999**, *56*, 795–802. [CrossRef]
72. Jessop, B.M. Geographic Effects on American Eel (*Anguilla Rostrata*) Life History Characteristics and Strategies. *Can. J. Fish. Aquat. Sci.* **2010**, *67*, 326–346. [CrossRef]
73. Vélez-Espino, L.A.; Koops, M.A. A Synthesis of the Ecological Processes Influencing Variation in Life History and Movement Patterns of American Eel: Towards a Global Assessment. *Rev. Fish Biol. Fish* **2010**, *20*, 163–186. [CrossRef]
74. Wood, C.M.; Farrell, A.P.; Brauner, C.J. *Homeostasis and Toxicology of Essential Metals*, 1st ed.; Elsevier: Amsterdam, The Netherlands, 2011; Volume 31A, ISBN 9780123786364.
75. Bornarel, V.; Lambert, P.; Briand, C.; Antunes, C.; Belpaire, C.; Ciccotti, E.; Diaz, E.; Diserud, O.; Doherty, D.; Domingos, I.; et al. Modelling the Recruitment of European Eel (*Anguilla anguilla*) throughout Its European Range. *ICES J. Mar. Sci.* **2018**, *75*, 541–552. [CrossRef]
76. Mouneyrac, C.; Leung, P.T.; Leung, K.M. Cost of Tolerance. In *Tolerance to Environmental Contaminants*; CRC Press: Boca Raton, FL, USA, 2011; pp. 265–298.
77. Freese, M.; Rizzo, L.Y.; Pohlmann, J.-D.; Marohn, L.; Witten, P.E.; Gremse, F.; Rütten, S.; Güvener, N.; Michael, S.; Wysujack, K.; et al. Bone Resorption and Body Reorganization during Maturation Induce Maternal Transfer of Toxic Metals in Anguillid Eels. *Proc. Natl. Acad. Sci. USA* **2019**, *116*, 201817738. [CrossRef]
78. Pierron, F.; Baudrimont, M.; Dufour, S.; Elie, P.; Bossy, A.; Baloche, S.; Mesmer-Dudons, N.; Gonzalez, P.; Bourdineaud, J.P.; Massabuau, J.C. How Cadmium Could Compromise the Completion of the European Eel's Reproductive Migration. *Environ. Sci. Technol.* **2008**, *42*, 4607–4612. [CrossRef]
79. van Ginneken, V.J.T.; van den Thillart, G.E.E.J.M. Eel Fat Stores Are Enough to Reach the Sargasso. *Nature* **2000**, *403*, 156–157. [CrossRef]
80. Kime, D.E. The Effects of Pollution on Reproduction in Fish. *Rev. Fish Biol. Fish* **1995**, *5*, 52–95. [CrossRef]
81. Vos, J.G.; Dybing, E.; Greim, H.A.; Ladefoged, O.; Lambré, C.; Tarazona, J.; Brandt, I.; Vethaak, A.D. Health Effects of Endocrine-Disrupting Chemicals on Wildlife, with Special Reference to the European Situation. *Crit. Rev. Toxicol.* **2000**, *30*, 71–133. [CrossRef] [PubMed]
82. Horri, K.; Alfonso, S.; Cousin, X.; Munschy, C.; Loizeau, V.; Aroua, S.; Bégout, M.L.; Ernande, B. Fish Life-History Traits Are Affected after Chronic Dietary Exposure to an Environmentally Realistic Marine Mixture of PCBs and PBDEs. *Sci. Total Environ.* **2018**, *610–611*, 531–545. [CrossRef]
83. Bastos Gonçalves, B.; Cardoso Giaquinto, P.; dos Santos Silva, D.; de Melo e Silva Neto, C.; Alves de Lima, A.; Antonio Brito Darosci, A.; Laço Portinho, J.; Fernandes Carvalho, W.; Lopes Rocha, T. Ecotoxicology of Glyphosate-Based Herbicides on Aquatic Environment. In *Biochemical Toxicology—Heavy Metals and Nanomaterials*; IntechOpen: London, UK, 2019.
84. Hendry, A.P.; Farrugia, T.J.; Kinnison, M.T. Human Influences on Rates of Phenotypic Change in Wild Animal Populations. *Mol. Ecol.* **2008**, *17*, 20–29. [CrossRef] [PubMed]